JMATPRO	Journal of Advanced Materials and Processing 11 (1): 25-40, Winter 2023 http://sanad.iau.ir/journal/jmatpro doi: 10.71670/jmatpro.2024.981647

Research Paper

Continuous Grain Refinement of Pure Aluminum During Cyclic Contraction/Expansion Extrusion (CCEE) Analyses by Micromechanical-Based FE and Experimental Methods

Hossein Jafarzadeh[1*], Sina Hassan Alipouri Fard[1], Alireza Babaei[2]

1. Department of Mechanical Engineering, Tabriz Branch, Islamic Azad University, Tabriz, Iran

2. Department of Mechanical Engineering, Technical and Vocational University (TVU), Tehran, Iran

ARTICLE INFO

Article history:

Received 08 September 2023
Accepted 2 December 2023
Available online 1 Febryary 2023

Keywords:
Severe plastic deformation
Cyclic extrusion contraction/expansion
Finite element analysis
Aluminium

ABSTRACT

Severe plastic deformation (SPD) has become an efficient route for producing ultrafine-grained and nanostructured high-strength metallic materials. The present study investigates the feasibility of synthesizing rod-shaped nanostructured pure aluminium samples with the newly presented severe plastic deformation (SPD) method called cyclic contraction/expansion extrusion (CCEE). Also, the deformation characteristics of this process were studied using both micromechanical-based finite element simulations and experimental methods. Tensile test results showed a noticeable increase in yield and ultimate tensile strength values to 155 MPa and 191 MPa from the initial values of 56 MPa and 112 MPa, respectively, after the second pass of CCEE processing. The microhardness measurements showed a significant increase in hardness values to 61 Hv from the initial value of 27 Hv at the end of the first and second passes of CCEE. Results showed that the proposed technique is an efficient SPD method capable of imposing severe stains in the order of 20 after six repeated cycles. The constitutive micro-mechanical approach was implemented to predict microstructure evolution during CCEE processing. The UFG cylindrical aluminium samples with a mean grain size of 480 nm at the end of the first pass and 360 nm at the end of the second pass of CCEE were processed from the initial grain size of ~55 μm. The XRD-obtained grain sizes were consistent with the FEM-predicted values.

Citation: Jafarzadeh, H.; Hassan Alipouri Fard, S.; Babaei, A. (2023). Continuous Grain Refinement of Pure Aluminum During Cyclic Contraction/Expansion Extrusion (CCEE) Analyses by Micromechanical-Based FE and Experimental Methods, Journal of Advanced Materials and Processing, 11 (1), 25-40. doi: 10.71670/jmatpro.2024.981647

[*] **Corresponding Author:**
E-Mail: h.jafarzadeh@iaut.ac.ir

1. Introduction

Ultrafine-grained and nanostructured metallic materials have unique physical, chemical, and mechanical properties compared with their coarse-grained counterparts [1-3]. Also, it has been demonstrated that grain refinement improves both strength and ductility of metallic materials [4, 5]. So far, different processing routes have been introduced for grain refinement, divided into two categories: top-down and bottom-up approaches. The "Bottom-up" approach is related to techniques that produce Nanostructured materials by assembling atoms or consolidating Nano-powders. These techniques include electro-deposition [6], ball milling, and subsequent consolidation with hot isostatic pressing [7]. Nevertheless, these techniques are limited to the production of small samples which can be utilized in some fields such as electronic devices. The ''top-down'' approach is different because it depends upon taking a bulk solid with a relatively coarse grain size and processing the solid to produce an ultrafine-grained microstructure through heavy straining or shock loading [8]. Severe plastic deformation is an efficient route for the production of ultrafine-grained and nanostructured materials. In this approach, a limited strain is imposed on the sample in each step, and sample dimensions remain unchanged so that the process can be repeated to impose the desired plastic strain levels [8]. So far, different techniques have been introduced and used on a laboratory scale to produce nanostructured metals and alloys. These processing methods are equal channel angular pressing (ECAP) [8], accumulative roll bonding (ARB) [9], high-pressure torsion (HPT) [10], tube reverse extrusion (TRE) [11], repetitive tube expansion and extrusion (RTES) [12], cyclic extrusion compression (CEC) [13], cyclic extrusion expansion (CEE) [14]. The study of microstructure evolution is essential since the macroscopic mechanical properties, such as yield and ultimate tensile strength, elongation, etc., are related to the grain size and distribution [15]. Depending on the stacking fault energy (SFE) of the material, the microstructure evolves through continuous dynamic recrystallization (CDRX) or discontinuous dynamic recrystallization (DDRX) [15]. In aluminium with a high SFE value, recrystallization occurs gradually and continuously during plastic flow [15, 16]. By imposing effective plastic strain (EPS) at the beginning of SPD processes, the density of dislocations inside the primary grains gets higher values, and an intra-granular microstructure is formed [17]. The CDRX is commenced as the imposed plastic strain increases by misorientation of dislocation intra-granular structure and creation of sub-grains with high-angle and distinguishable boundaries inside the primary structure [18]. Many researchers implemented the finite element method as an essential technique for analyses of different SPD processes on the macroscopic scale [19, 20]. Nonetheless, most FEM analyses have been conducted on a macroscopic scale and have not considered the microstructure parameters such as grain size and dislocation density. Kim et al. implemented a dislocation density-based model, which was proposed by Estrin [20] to predict the cell size and accumulation of dislocation during ECAP processing of Al samples using the FE method. A micromechanical-based constitutive model was introduced by Hallberg et al. for the prediction of grain size and dislocation density during ECAP of AA1050 alloy [15].

In this study, the feasibility of the synthesis of pure Al is investigated with the CCEE method. The process is analyzed at the macro level by the FE method. Also, the microstructure evolution (grain size and dislocation density) was simulated in the FE framework based on a constitutive model presented in Ref. [15].

2. Finite element and experimental procedure

The cylindrical pure aluminum samples were prepared from the as-cast ingot and annealed for 3 hours at 350 °C. The principle of the CCEE process is shown schematically in Fig. 1.

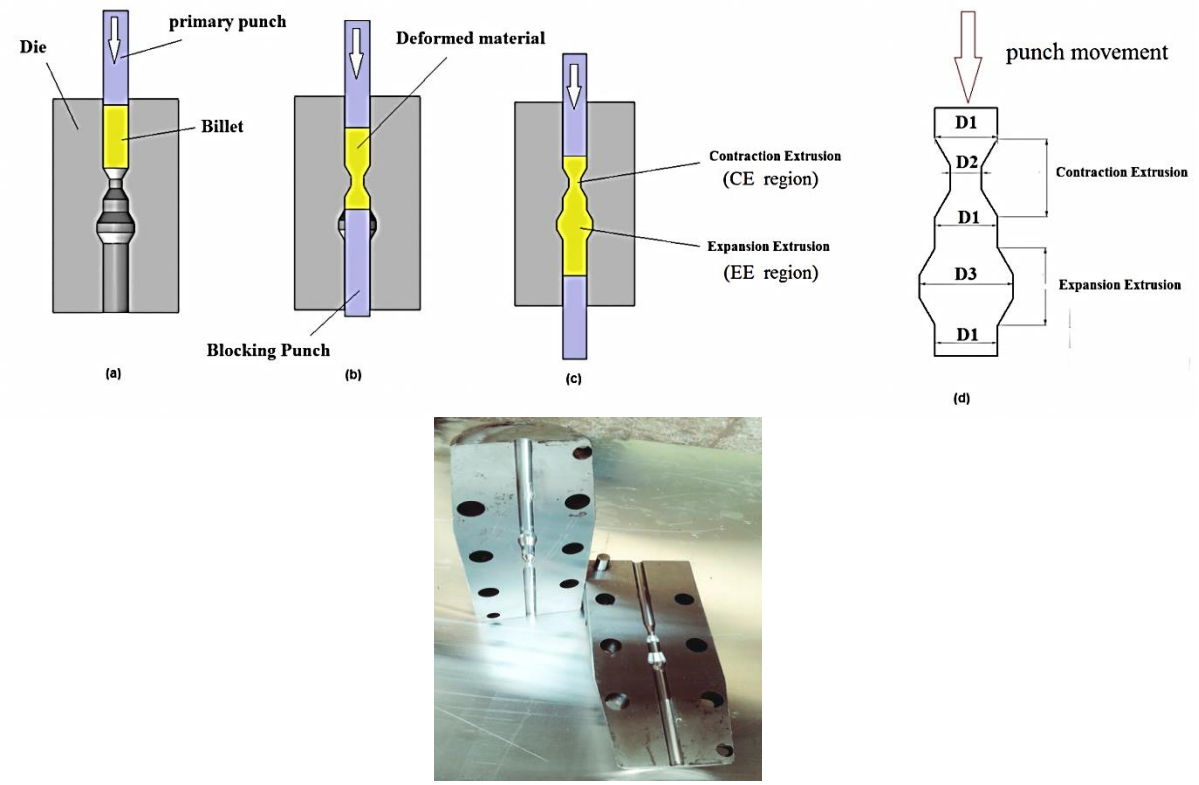

Fig. 1. Schematic illustration of CCEE and the prepared die set [21]

As is seen in Fig. 1, the die channel geometry of CCEE includes two separate regions entitled contraction extrusion and expansion extrusion. During deformation by contraction extrusion, the diameter of the cylindrical sample is decreased from D_1 to D_2 and then increased to D_1 again. In the next region, the diameter of the sample is increased from D_1 to D_3 and then decreased to D_1 again. As illustrated in Fig. 1, it is possible to increase the imposed plastic strain by reversing the press direction after the completion of each pass. The magnitude of accumulated plastic strain imposed by CCEE was equal to [21]:

$$\varepsilon_{total} = N(\varepsilon_{contraction} + \varepsilon_{expansion}) \quad (1)$$

where N is the number of CCEE deformation passes and other equation is presented as follows:

$$\varepsilon_{contraction} = 4\ln(\frac{D_1}{D_2}) \quad (2)$$

$$\varepsilon_{expansion} = 4\ln(\frac{D_3}{D_1}) \quad (3)$$

Considering the D_1, D_2, and D_3 to 10, 5.8, and 14.2 mm, the total accumulated effective plastic strain in one cycle of CCEE processing is equal to 3.6. The X-ray diffraction (XRD) method is implemented to study microstructure evolution. Cu-kα radiation with the step of 0.025° in a range of 10°-80° is used to extract the profile patterns of the processed sample. The Williamson-Hall analysis was used to interpret XRD-obtained profiles as follows:

$$FWHM \ \cos\theta = \frac{k\lambda}{D} + 4\varepsilon Sin\theta \quad (4)$$

where the wave's full width at half maximum is referred to as FWHM, the diffraction angle is θ, k is constant, D is the crystallite size, λ is the wavelength, and ε is the lattice micro-strain. The evolution of dislocation density (ρ) could be calculated as follows [22, 23]:

$$\rho = (\rho_t \times \rho_s)^{1/2} \quad (5)$$

Where:

$$\rho_t = \frac{3}{D^2} \quad (6)$$

$$\rho_s = \frac{6\pi\varepsilon^2}{b^2} \quad (7)$$

In which b is the Burgers vector.

To study the evolved microstructure of processed samples, they were cut and then the surfaces were prepared using standard metallographic techniques. The specimen was prepared for microstructural investigations and then was mechanically ground and polished. Subsequently, electro-polishing with a solution of 30% HNO_3 in methanol at -40 °C was utilized in the preparation of the specimens for microscopic studies. Vickers micro-hardness method was implemented to measure the hardness variations during the different cycles of CCEE. Also, a uniaxial tensile test is conducted to quantify yield strength (Y.S.), ultimate tensile strength (UTS), and elongation (EL%) of samples.

In the present investigation, FEM was utilized to study different aspects of the plastic flow of pure aluminium during processing with the integrated CCEE technique. So, the cylindrical aluminium sample was assumed to be a deformable material, and the tools were assumed to be rigid parts. The initial cylindrical sample was discretized by 32000 tetrahedron elements. Fig. 2 shows the sample position inside the die channel and the meshed specimen just before deformation. The friction coefficient of die and billet interaction surfaces was assumed to be 0.1.

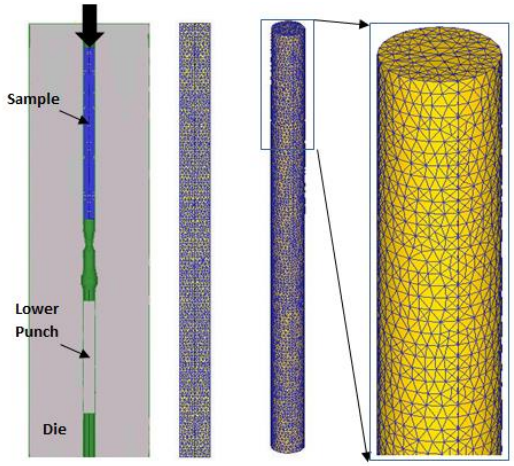

Fig. 2. Schematic of the sample position inside die channel and the meshed sample just before deformation.

The micromechanical analysis in the FEM environment was based on the constitutive model proposed in Ref. [15]. The microstructure of pure aluminium evolved through continuous dynamic recrystallization (CDRX) [15, 16]. In the proposed constitutive model, the average grain size (D) and dislocation density (ρ_d) were introduced as micromechanical parameters, which evolve during CDRX and correspond to the evolution of effective plastic strain (ε_{eff}^{pl}) in macro-scale simulations. The variation of average grain size (D) is related to ε_{eff}^{pl} the following exponential equation [24]:

$$D = D_0 - [D_0 - z_1 \exp(-z_2 \varepsilon_{eff}^{pl})][1 - \exp(-z_3 \langle \varepsilon_{eff}^{pl} - \varepsilon_c^{pl} \rangle^{z_4})] \quad (8)$$

where D_0 is the initial average grain size, zi referred to as recrystallization speed parameters [24], ε_c^{pl} denoted the critical plastic strain in which CDRX starts and has an amount of 0.1 for pure aluminium [15]. The accumulation of dislocation density, ρ_d, during CCEE processing could be predicted as follows [24]:

$$\frac{\dot{\rho_d}}{\rho_d^0} = \left[d_1 \sqrt{\frac{\rho_d}{\rho_d^0}} - d_2 \frac{\rho_d}{\rho_d^0} + d_3 \frac{D_0}{D} \right] \dot{\varepsilon}_{eff}^{pl} \quad (9)$$

The equation has three different terms for the evolution of ρ_d, including the dislocation generation by the Frank-Read mechanism denoted by d_1, the dislocation annihilation through dynamic recovery referred by d_2, and the effects of grain size by parameter d_3. According to the Hall-Petch equation, the macroscopic mechanical properties, such as yield stress σ_y is related to the micromechanical quantities, including grain size D and dislocation density ρ_d. Therefore, in the present study, the yield stress of material during CCEE is related to the microstructure parameters D and ρ_d and is defined as [24]:

$$\sigma_y(\rho_d, D) = \sigma_{y0} + H\left(\sqrt{\frac{\rho_d}{\rho_{d0}}} - 1\right) + k_D\left(\sqrt{\frac{D_0}{D}} - 1\right) \quad (10)$$

where the Peierls stress is denoted as σ_{y0}, the hardening modulus is referred to as H, and the stress intensity factor is k_D. The values of these parameters are shown in Table 1 [24]:

Table 1. Material parameters used in the proposed model [15, 24]

Parameter	Value	Description
σ_{y0}	56 MPa	Initial yield stress
H	0.96 MPa	Isotropic hardening modulus
K_D	4.3 MPa	Stress intensity factor in the Hall-Petch relation
ρ_d^0	$1\times10^9 m^{-2}$	Initial dislocation density
d_1	279.5	Controlling parameter (creation of dislocations)
d_2	7.7	Controlling parameter (annihilation of dislocations)
d_3	437.5	Controlling parameter (influence of grain size on the dislocation density)
D0	55 μm	Initial average grain size
K	56 GPa	Bulk modulus
G	27 GPa	Shear modulus
ε_c^{pl}	0.1	Critical plastic strain

3. Results and discussion

3.1. Microstructure evolution and mechanical properties

The cross-section of the CCEE-processed samples was examined for microstructural observations. The initial annealed aluminium sample with an average grain size of ~55 μm is fed through the CCEE die channel (Fig. 3). Besides, Fig. 4a,b depict the processed microstructure of the CCEE processed specimens at the end of first and second passes, respectively. The total accumulated effective plastic strain (EPS) into the material plays a prominent role in grain refinement during SPD processes [8, 21]. As is calculated analytically in a previous study by the authors [21], the total accumulated EPS in each pass of CCEE is about 3.6.

As shown in Fig. 4, the initial microstructure of Al samples remarkably evolved after processing by the CCEE technique. This evolution of microstructure in Al alloys is mainly done through continuous dynamic recrystallization (CDRX). During CDRX and at the early stages of plastic deformation, the density of dislocation inside the large grains increases. So, the network of tangled dislocations forms the smaller grains with low-angle boundaries inside the initial larger grains. By the accumulation of effective plastic strain (EPS) in the structure through CCEE processing, the low-angle boundaries of the mentioned sub-grains got a new orientation to form ultra-fine grains with high-angle boundaries [25-27] .

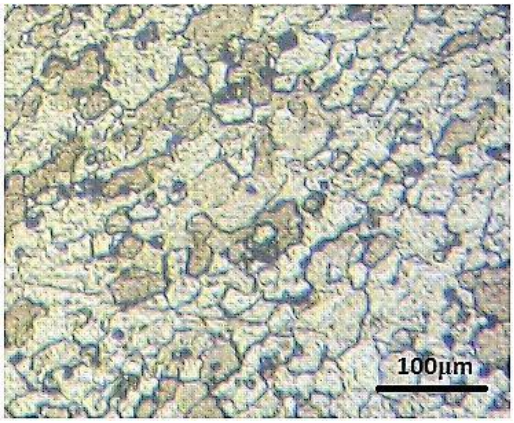

Fig. 3. The initial microstructure of pure aluminium [11].

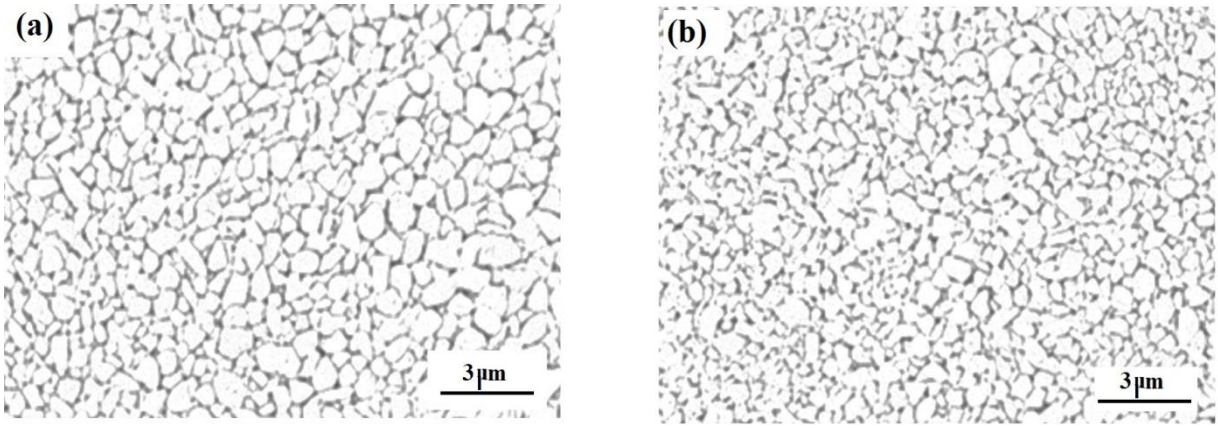

Fig. 4. The microstructure of CCEE processed pure aluminium at the end of (a) first and (b) second pass

Fig. 5 illustrates the XRD patterns for the initial and CCEE-processed samples. As is apparent from Fig. 5, crystalline planes of (220), (200), and (111) have intense diffractions. Therefore, based on these diffraction profiles, the Williamson-Hall technique is implemented to obtain the crystalline size of the CCEE-processed sample. The results showed an average crystalline/sub-grain size of ~480 nm at the end of the first pass of CCEE and ~360 nm at the end of the second pass. Hence, it is evident that the CCEE technique can fabricate materials with ultra-fine grain microstructure. The imposed shear strains and subdivision of dislocations through continuous dynamic recrystallization (CDRX) are two main mechanisms of grain refinement in Al alloys with high stacking fault energy (SFE) values [15, 16].

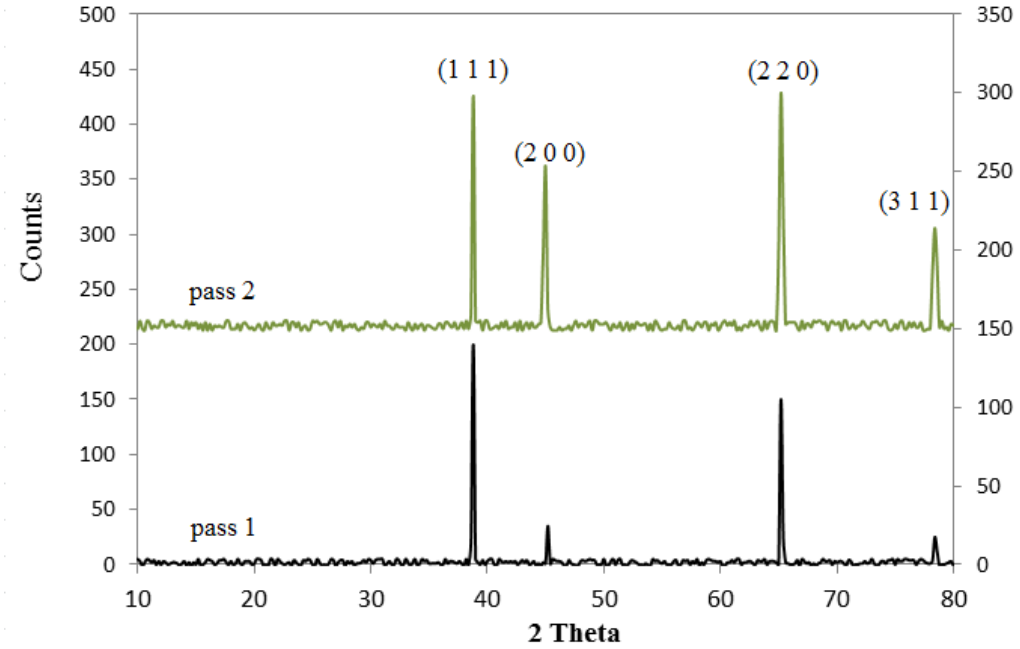

Fig. 5. The patterns of XRD for CCEE processed sample in first and second pass

The evolution of grain size through CDRX is a continuous and gradual process where the density of dislocations is increased in the structure at the beginning of plastic deformation. By increasing imposed EPS values, the networks of dislocation cells with low-angle boundaries are formed inside the primary coarse grains [28]. Furthermore, the cells are misoriented by the increase in plastic deformation, and new ultra-fine grains with distinguishable boundaries are formed [29]. Fig. 6 shows the documented tensile test results for the initial and processed samples at room temperature.

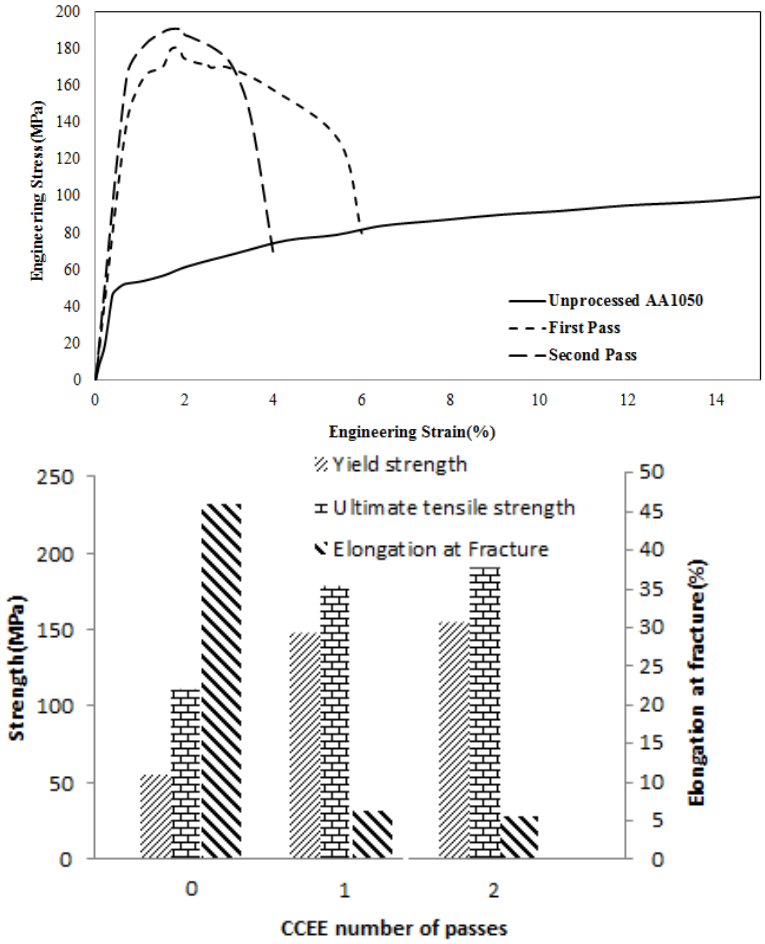

Fig. 6. Tensile test results

As is clearly seen from Fig. 6, the strength values are remarkably increased by the increase in the CCEE pass number. According to the Hall-Petch relation, the refinement of grain and accumulation of dislocations are two main parameters affecting strength increases [20]. As is evident from Fig. 6, the yield strength of the as-annealed sample is increased by a factor of 3.3, and the ultimate tensile strength is increased by a factor of 1.6 at the end of the first pass. Nevertheless, the elongation to fracture of the CCEE processed samples decreased to 6.3% from the initial value of 46% at the end of the first pass. The increase in strength in the first pass occurred with a greater slope than in subsequent passes, while in the following passes, this slope was less. According to Fig. 7, the value of Vickers microhardness is increased sharply at the end of the first pass, where the value of ~54 Hv is obtained from the initial amount of ~27 Hv. By increasing the CCEE number of passes, the accumulated EPS and Hv value are also increased. As is reported by the previous research, the values of hardness, EPS, and strength in SPD processing of aluminium alloys are directly related to each other based on the well-known Hall-Petch relation [9, 20].

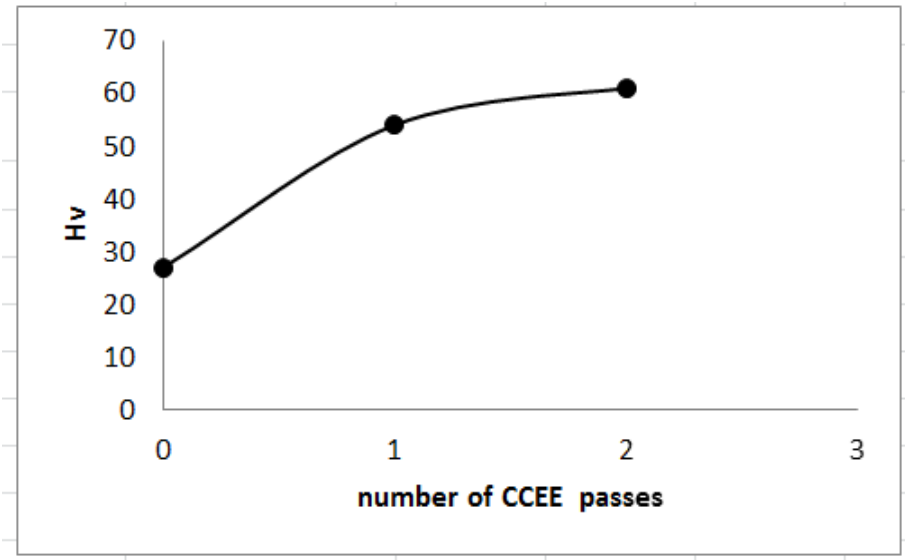

Fig. 7. Microhardness and EPS variation of CCEE processed Al sample

3.2. Plastic strain distribution

Fig. 8 shows the equivalent plastic strain distribution inside the sample after different passes of the CCEE process. As seen, plastic strain is distributed non-uniformly inside the sample; that is the nature of the deformation processes. Plastic strain is higher at near-surface regions compared to the sample's centre. This difference is due to the redundant shear strain imposed on near-surface regions due to friction between the sample's surface and the die channel wall. Fig. 8a represents the plastic strain distribution after the initial pass of the CCEE process. In this step, the cylindrical sample is pressed into the die channel by the upper punch. Therefore, the sample is extruded in the contraction extrusion region and reaches the bottom punch. After that, the material fills the die channel by continuing to press the sample. Hence, the material is subjected to expansion at the downside of the die channel. As can be seen, the amount of plastic strain at the contraction-extrusion region is in the range of 0.8-1.6 (blue colour). Also, the plastic strain in the order of 2.6-3.6 is imposed on the sample at the expansion extrusion region. Fig. 8b shows strain distribution after the first pass of this deformation process. The amount of plastic strain at the lower side of the sample is equal to 2, which is distinguished by its blue colour. This region of the sample is subjected only to contraction extrusion. The amount of plastic strain is increased by moving from the bottom to the topside of the sample. So, the amount of strain reached 3.8, which is shown by the yellow colour. Therefore, it can be said that this region of the sample is subjected to both contraction extrusion and expansion extrusion. Also, the strain level at near-surface regions is higher than the inside regions. The amount of plastic strain at each region of the sample is increased with increasing deformation steps. Furthermore, it can be seen that the plastic strain distribution after the third (Fig. 8d) and fifth (Fig. 8f) steps is similar to the strain distribution after the first step. Fig. 8c represents the plastic strain distribution inside the sample after the process's second pass. As it is evident, the plastic strain at the topside of the sample is lower than in other regions. The magnitude of the plastic strain is increased by moving from the top to the downside of the sample up to the contraction extrusion region. Also, the strain level increases when moving from the centre to near-surface regions. In addition, it can be seen that the strain distributions after the fourth (Fig. 8e) and sixth (Fig. 8g) passes are similar to the strain distribution after the second pass. It can be said that after each pass of cyclic contraction/expansion extrusion, the amount of plastic strain at the lower and upper sides of the sample is negligible compared with other regions. Also, the strain level is increased by moving toward deformation zones (expansion and contraction regions).

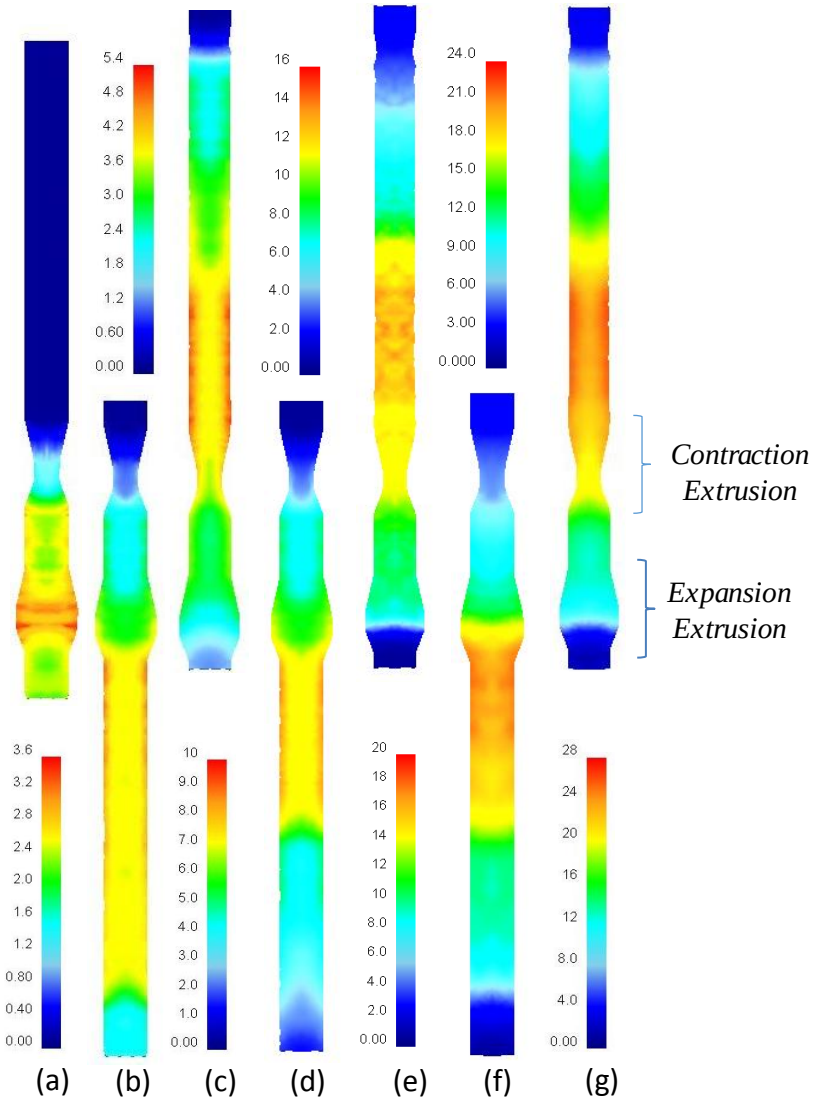

Fig. 8. Equivalent plastic strain distributions inside deformed sample after different passes: a) Initial step, b) step 1, c) step 2, d) step 3, e) step 4, f) step 5 and g) step 6.

Fig. 9a shows the variation of plastic strain through the centerline of the sample after the first, third and fifth passes. As can be seen, the two ends of the sample experienced a lower strain than the strain in the middle. This trend also exists in the plastic strain variations after the second, fourth, and sixth passes, as shown in Fig. 9b. The variations of maximum strain at the centerline (ε_m) with deformation passes are also seen in Fig. 9. It can be said that the variations in maximum strain with deformation passes are near linear. So, the maximum strain of 25 is achieved after the sixth pass.

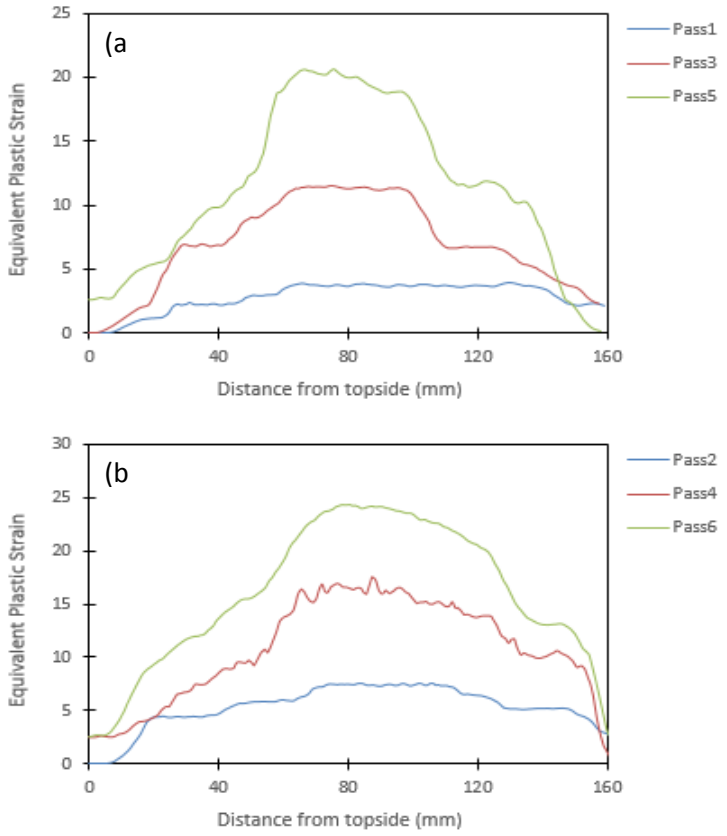

Fig. 9. Variations of equivalent plastic strain along centerline of sample after different deformation passes: a) first, third, and 5th passes, and b) second, 4th and 6th passes.

3.3. Damage accumulation

Some materials, called difficult-to-work materials, are prone to forming surface cracks during severe plastic deformation like equal channel angular pressing [30]. Therefore, a limited amount of plastic strain can be applied to these materials due to fracture at higher deformation passes. In this regard, some fracture criteria were proposed by researchers, but the Craft-Latham criterion has been used extensively for the prediction of the occurrence of fracture during plastic deformation of metallic materials. According to the Craft-Latham criterion, the fracture occurs when the tensile strain energy exceeds a critical value. The Craft-Latham damage is calculated using the following expression [30]:

$$D = \int_0^{\varepsilon_F} \frac{\sigma_T}{\bar{\sigma}} d\bar{\varepsilon} \qquad (1)$$

where ε_F is the strain at the fracture point, σ_T is the maximum tensile stress, $\bar{\sigma}$ is equivalent stress. The damage value is increased during metalworking processes by increasing plastic strain. Therefore, the maximum damage is achieved at the end of the deformation or when a crack is initiated at a specific region. Fig. 10 shows the distributions of Craft-Latham damage in the deformed sample after different passes of the CCEE process. As can be seen, after the initial step (Fig. 10a), the damage value is almost zero for the whole part of the sample except the contraction extrusion region. At this region, the damage value is increased from the centre to near-surface regions. After completion of the first step (Fig. 10b), it is seen that the damage value is zero at regions before the contraction extrusion zone, regions inside the contraction extrusion zone, regions between contraction extrusion and expansion extrusion zones, and regions inside the expansion extrusion zone. Nevertheless, the value of the damage factor is increased at the deformed part of the sample just after the expansion extrusion zone. Therefore, it is evident that the damage value is increased with increasing plastic strain. Some regions of the sample, which have not been subjected to plastic deformation during the first pass, are deformed during the second pass, and the damage factor is increased simultaneously. Therefore, the damage value is non-zero at all regions of the sample

after conducting the second pass. The damage value is increased with increasing deformation steps, and the maximum damage is achieved after imposing six deformation passes which is represented by the red color in Fig. 10.

.

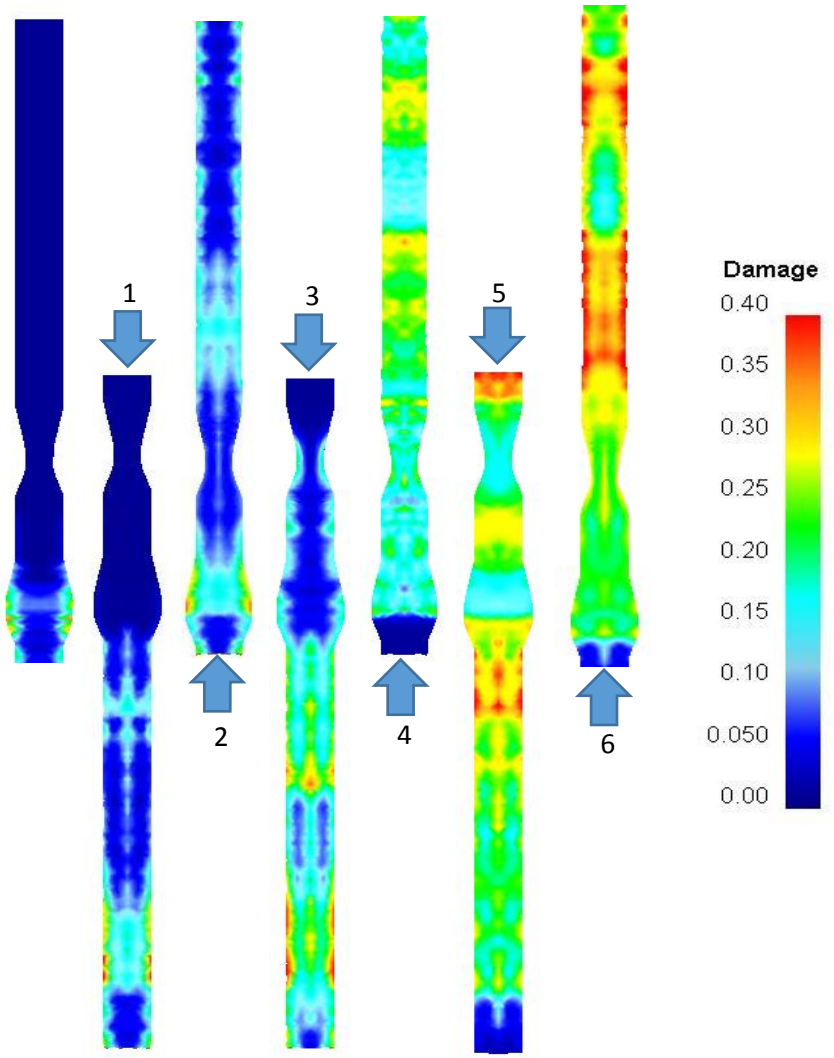

Fig. 10. Craft-Latham damage distributions inside sample after different deformation passes.

The variations of damage factor along the centerline of the deformed sample after each deformation passes are also shown in Fig. 11. As can be seen, the damage value is zero through the 60 mm of the topside of the centerline, and only the bottom side has non zero damage. After the second pass, the damage value is none zero at every point along the centerline. It is demonstrated that the damage value is increased through the centerline with increasing deformation passes. Fig. 12 represents the variation of maximum damage along the sample centerline with deformation passes. As it is seen, the maximum damage is increased with increasing deformation passes and reaches 0.4 after six passes.

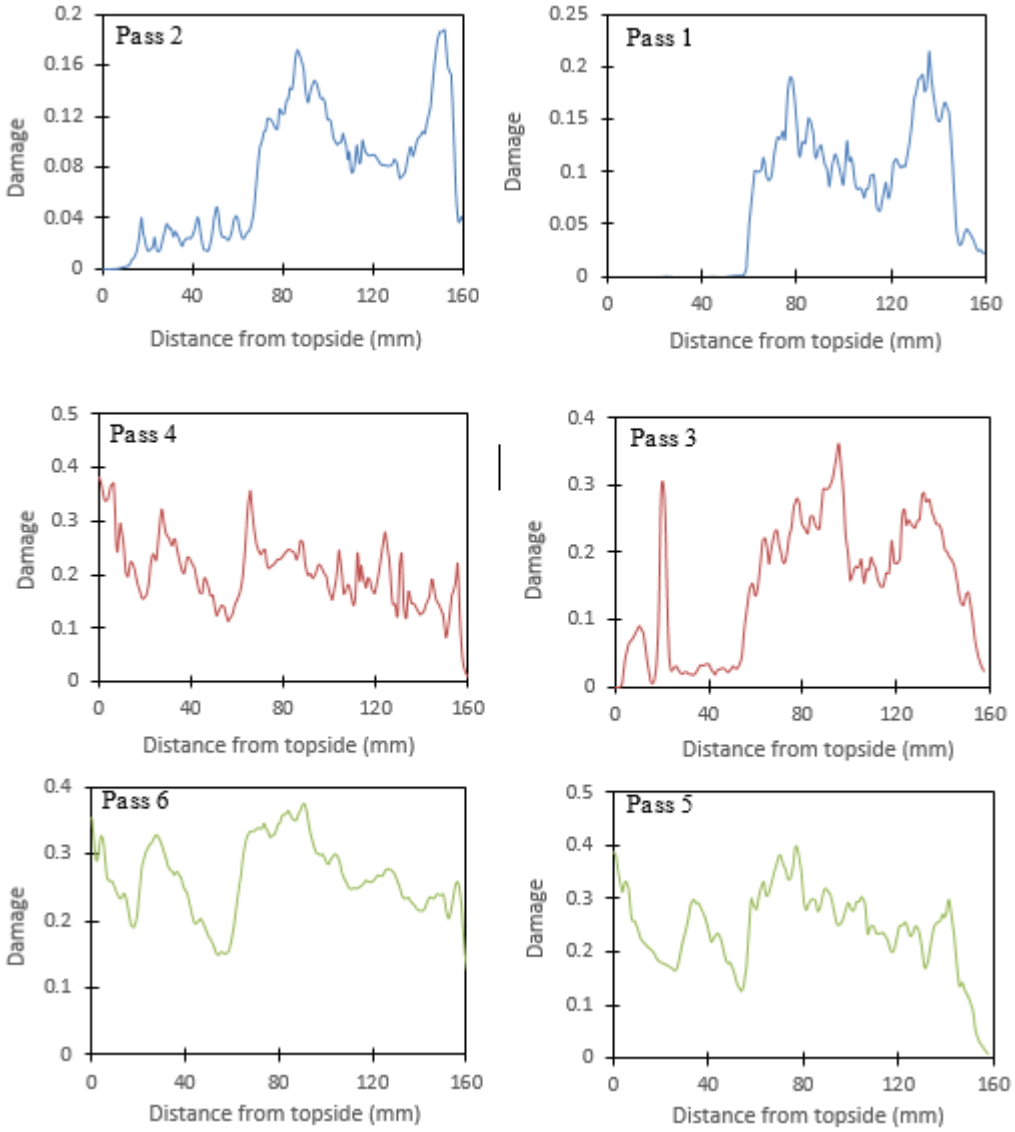

Fig. 11. Variations of damage factor along centerline of sample after different deformation passes.

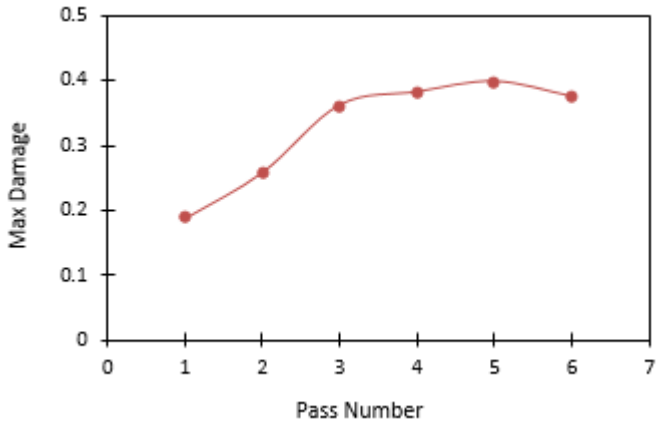

Fig. 12. Variations of maximum damage factor with deformation passes.

3.4. Equivalent Stress distribution

Fig. 13 shows distributions of equivalent stress inside the deformed sample after deformation passes of 1, 3, and 5. As can be seen, stress is none zero at the deformation zones of contraction extrusion and expansion extrusion. It is worth noting that the equivalent stress distributions after deformation passes of 2, 4, and 6, is similar to 1, 3, and 5 passes.

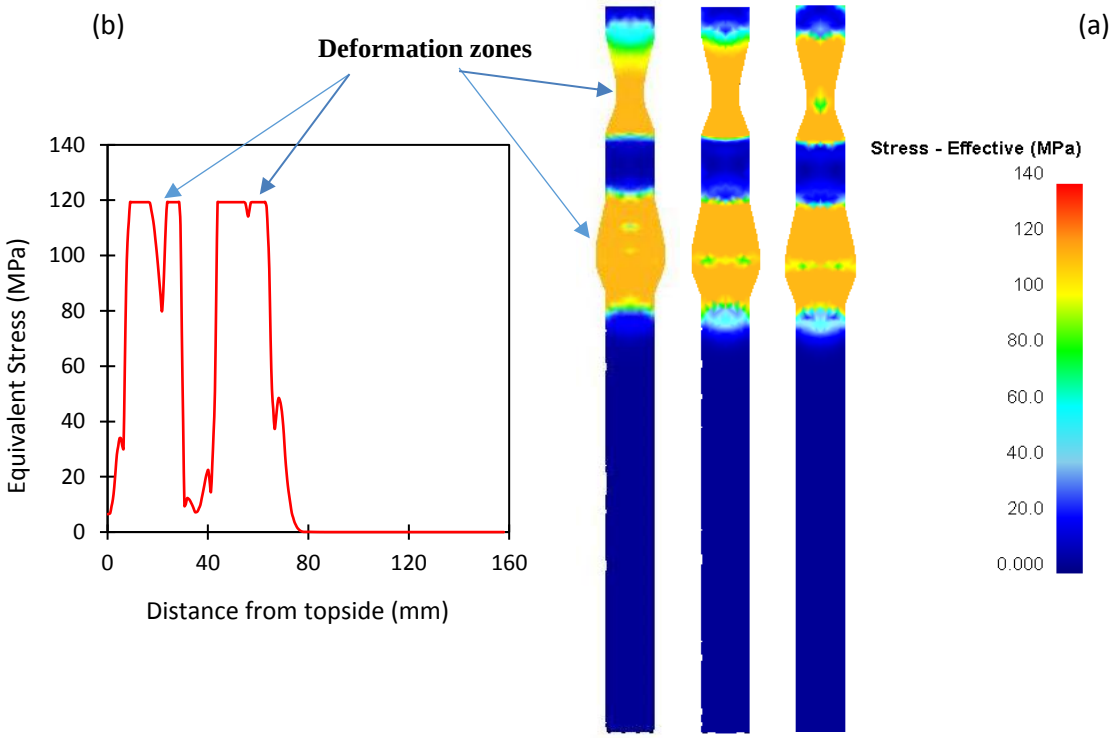

Fig. 13. a) Equivalent stress distribution inside sample after deformation passes of 1, 3 and 5, and b) variations of equivalent stress along centerline of sample.

3.5. Pressing Force

The pressing force required for the compilation of each deformation pass is shown in Fig. 14. During the initial step (Fig. 14a), the pressing force is increased to 4 KN and remains constant until the end of a sample is reached by to bottom punch. At this time, the pressing force is increased gradually and reaches 8 KN at the end of the initial step. During the first pass, as shown in Fig. 14b, the pressing force of 11 KN is required to impose plastic deformation on the sample. The fluctuations observed in pressing force during simulation are expected and have been reported in some studies [30]. Fig. 14c shows the variations of pressing force during the second deformation pass. The initial pressing force is 8 KN and increased to 10 KN at the end of the deformation. It is seen that variations of pressing force are similar during each odd step (1, 3, and 5) and also during each even step (2, 4, and 6).

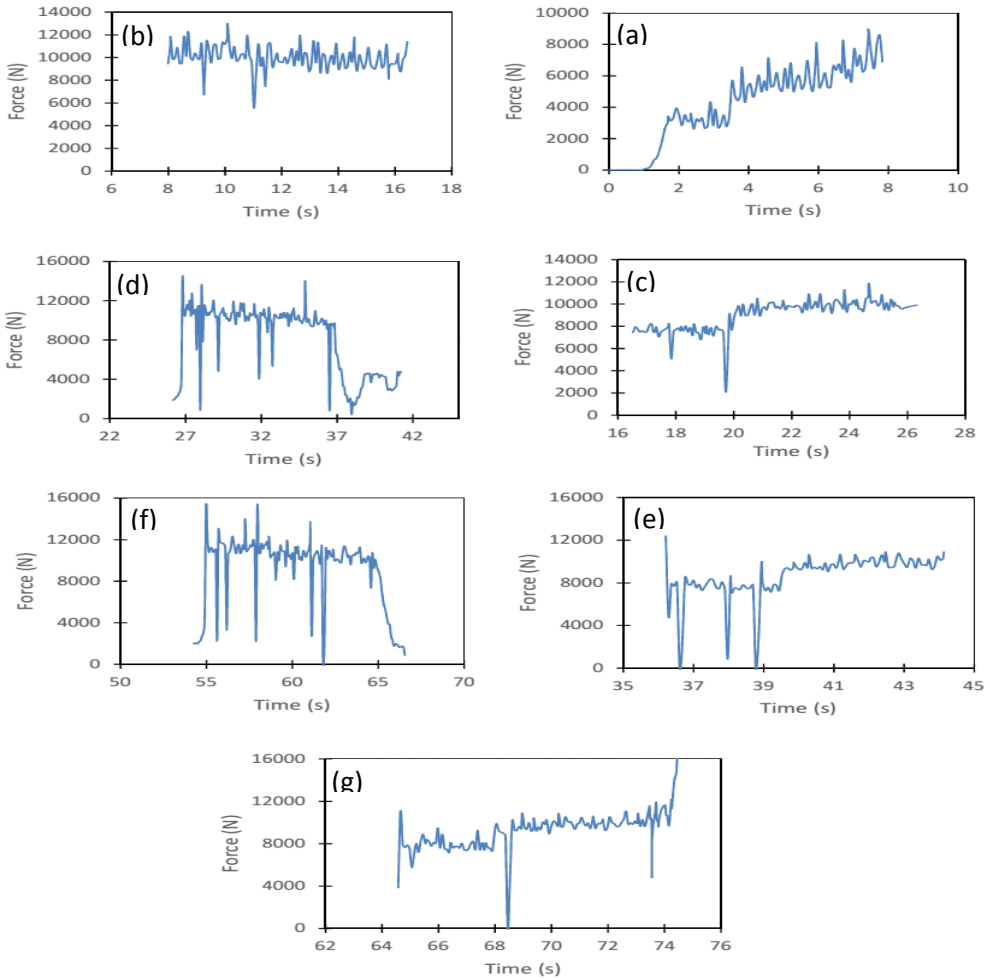

Fig. 14. Variations of pressing force during deformation of Cu at different steps: a) Initial step, b) 1st step, c) 2nd step, d) 3rd step, e) 4th step, f) 5th step, and g) 6th step.

3.6. Grain size and dislocation density

The grain size and dislocation density as microstructural parameters significantly affect the macroscopic properties of material, such as yield strength, ultimate tensile strength, elongation, etc. Therefore, considering the effect of these parameters on the material properties will be of great importance in the FE simulation of plastic deformation processes. Therefore, in this study, the evolution of two parameters of grain size and dislocation density in FE simulation was considered, and the results are shown in Fig. 15. As is shown in Fig. 14, the annealed aluminum with the initial grain size of D_0= 55μm and dislocation density of $\rho_0 = 1\times10^{9}m^{-2}$ is placed inside the CCEE die assembly. By applying punch pressure, the material flows in the die channel and enters the deformation areas named expansion extrusion and contraction extrusion. As it passes through these deformation areas, the material's microstructure undergoes a plastic deformation of 3.6 at the end of the first pass. As it is clear, applying a higher amount of plastic deformation has an effective role in changing the grain size and increasing the dislocation density [3]. As seen in Fig. 15, there is minimum grain size and maximum dislocation density in areas close to the shear bands. As the plastic deformation continues in the die channel of CCEE, the grain size decreases gradually, and the dislocation density increases. At the end of the first and second pass, the grain size reaches 480nm and the dislocation density $\rho = 2.2\times10^{12}m^{-2}$, respectively. The results of FE simulations are in good agreement with the results of the XRD experimental analysis.

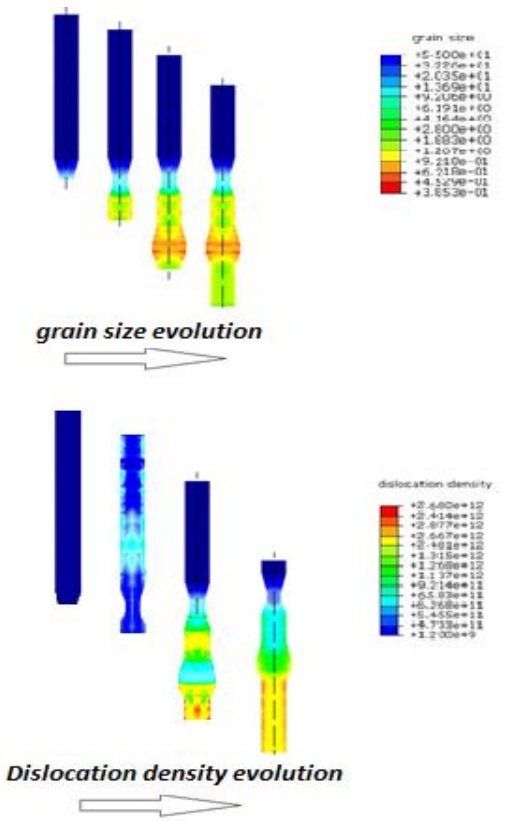

Fig. 15. Grain size and dislocation density evolution during first pass of CCEE

4. Conclusions

In the present investigation, a new method of severe plastic deformation called cyclic contraction/expansion extrusion was proposed to fabricate UFG pure aluminum and the following conclusions have been made:

1- The UFG cylindrical aluminum samples with a mean grain size of 480 nm at the end of the first pass and 360 nm at the end of the second pass of CCEE were processed from the initial grain size of ~55 μm.

2- The predicted grain size values are in good agreement with the XRD-obtained results.

3- The yield strength, ultimate strength, and microhardness were increased to 155 MPa, 191 MPa, and 61 Hv from the initial values of 56 MPa, 112 MPa, and 27 Hv, respectively, after the second pass of CCEE processing.

4- Maximum amount of imposed plastic strain is increased with deformation passes and reaches 25 after six steps. Therefore, this processing technique has high efficiency for the production of ultrafine-grained and nanostructured metallic materials.

5- The damage factor increases with the accumulation of deformation and reaches 0.4 in some regions after six passes of plastic deformation.

6- It is inferred from the variations of pressing force during each deformation step that the maximum pressing force needed to conduct cyclic contraction/expansion extrusion on pure Aluminum is about 12 KN.

References

[1] M.J. B. Hadzima, Y. Estrin, H. S. Kim, "Microstructure and corrosion properties of ultrafine-grained interstitial free steel", Materials Science and Engineering A, , Vol. 462, No. 2007, pp. 243-247.

[2] A. Zhilyaev, K. Oh-Ishi, T. Langdon, T. McNelley, "Microstructural evolution in commercial purity aluminum during high-pressure torsion", Mater Sci Eng A, Vol. 277, No. 2005, pp. 410–411.

[3] A.P. Zhilyaev, T.G. Langdon, "Using high-pressure torsion for metal processing: Fundamentals and applications", Prog. Mater. Sci., Vol. 53, No. 6, 2008, pp. 893-979.

[4] J.J. A. Ma, N. Saito, I. Shigematsu, Y. Yuan, D. Yang, Y. Nishida, "Improving both strength and ductility of a mg alloy through a large number of ecap passes", Materials Science and Engineering A,, Vol. 513-514, No. 2009, pp. 122-127.

[5] H. Jafarzadeh, M. Zadshakoyan, E. Abdi Sobbouhi, "Numerical studies of some important design factors in radial-forward extrusion process", Materials and Manufacturing Processes, Vol. 25, No. 8, 2010, pp. 857-863.

[6] L.Z. S. Xu, X. Zhang, C. He, Y. Lv, "Synthesis of ag2se nanomaterial by electrodeposition and its application as cataluminescence gas sensor material

for carbon tetrachloride", Sensors and Actuators B: Chemical,, Vol. 155, No. 2011, pp. 311-316.
[7] G.D. J. Gubicza, P. Szommer, B. Bacroix, "Microstructure and yield strength of ultrafine grained aluminum processed by hot isostatic pressing", Materials Science and Engineering A,, Vol. 458, No. 2007, pp. 385-390.
[8] R.Z. Valiev, T.G. Langdon, "Principles of equal-channel angular pressing as a processing tool for grain refinement", Prog. Mater. Sci., Vol. 51 No. 2006, pp. 881-981.
[9] N.T. Y. Saito, H. Utsunomiya, T. Sakai, R.G. Hong, "Ultra-fine grained bulk aluminum produced by accumulative roll-bonding (arb) process", Scr. Mater., Vol. 39, No. 1998, pp. 1221–1227.
[10] K.N. G. Sakai, Z. Horita, T. G. Langdon, "Developing high-pressure torsion for use with bulk samples", " Materials Science and Engineering A, , Vol. 406, No. 2005, pp. 268-273.
[11] H. Jafarzadeh, A. Babaei, "Tube reversing and extrusion (tre) as a novel method for producing ufg thin tubes", Transactions of the Indian Institute of Metals, Vol. 70, No. 4, 2017, pp. 979-988.
[12] H. Jafarzadeh, K. Abrinia, "Fabrication of ultra-fine grained aluminium tubes by rtes technique", Materials Characterization, Vol. 102, No. 2015, pp. 1-8.
[13] N. Pardis, B. Talebanpour, R. Ebrahimi, S. Zomorodian, "Cyclic expansion-extrusion (cee): A modified counterpart of cyclic extrusion-compression (cec)", Materials Science and Engineering: A, Vol. 528, No. 25, 2011, pp. 7537-7540.
[14] M. Richert, H.P. Stüwe, M.J. Zehetbauer, J. Richert, R. Pippan, C. Motz, E. Schafler, "Work hardening and microstructure of almg5 after severe plastic deformation by cyclic extrusion and compression", Materials Science and Engineering: A, Vol. 355, No. 1, 2003, pp. 180-185.
[15] H. Hallberg, M. Wallin, M. Ristinmaa, "Modeling of continuous dynamic recrystallization in commercial-purity aluminum", Materials Science and Engineering: A, Vol. 527, No. 4–5, 2010, pp. 1126-1134.
[16] H. Jazaeri, F.J. Humphreys, "The transition from discontinous to continous recrystallization in some aluminum alloys i- the deformed state.", Acta Mater., Vol. 52, No. 2004, pp. 3239-3250.
[17] T.G. Langdon, "The principles of grain refinement in equal-channel angular pressing", Mater Sci Eng A Vol. 462, No. 2007, pp. 3–11.
[18] K. Edalati, T. Fujioka, Z. Horita, "Microstructure and mechanical properties of pure cu processed by high-pressure torsion", Materials Science and Engineering: A, Vol. 497, No. 1–2, 2008, pp. 168-173.
[19] J. Suh, H. Kim, J. Park, J. Chang, " Finite element analysis of material flow in equal channel angular pressing", Scripta Mater, Vol. 44, No. 2001, pp. 677.
[20] H.S. Kim, Y. Estrin, M.B. Bush, "Plastic deformation behaviour of fine-grained materials", Acta Materialia, Vol. 48, No. 2, 2000, pp. 493-504.
[21] R.A. Peyghan, H. Jafarzadeh, "Study of fine-grained pure copper fabrication by cyclic contraction/expansion extrusion (ccee) using experimental and finite element simulation methods", Transactions of the Indian Institute of Metals, Vol. 72, No. 3, 2019, pp. 757-765.
[22] V.L. Niranjani, K.C. Hari Kumar, V. Subramanya Sarma, "Development of high strength al–mg–si aa6061 alloy through cold rolling and ageing", Materials Science and Engineering: A, Vol. 515, No. 1–2, 2009, pp. 169-174.
[23] P. Sahu, M. De, S. Kajiwara, "Microstructural characterization of stress-induced martensites evolved at low temperature in deformed powders of fe–mn–c alloys by the rietveld method", Journal of Alloys and Compounds, Vol. 346, No. 1–2, 2002, pp. 158-169.
[24] H. Hallberg, "Influence of process parameters on grain refinement in aa1050 aluminum during cold rolling", International journal of mechanical sciences, Vol. 66C, No. 2013, pp. 260-272.
[25] H. Hallberg, "Influence of process parameters on grain refinement in aa1050 aluminum during cold rolling", International Journal of Mechanical Sciences, Vol. 66, No. 2013, pp. 260-272.
[26] M.S. Mohebbi, A. Akbarzadeh, "Accumulative spin-bonding (asb) as a novel spd process for fabrication of nanostructured tubes", Materials Science and Engineering: A, Vol. 528, No. 1, 2010, pp. 180-188.
[27] A.P. Zhilyaev, G.V. Nurislamova, B.K. Kim, M.D. Baró, J.A. Szpunar, T.G. Langdon, "Experimental parameters influencing grain refinement and microstructural evolution during high-pressure torsion", Acta materialia, Vol. 51, No. 3, 2003, pp. 753-765.
[28] Z.J. Zhang, Q.Q. Duan, X.H. An, S.D. Wu, G. Yang, Z.F. Zhang, "Microstructure and mechanical properties of cu and cu–zn alloys produced by equal channel angular pressing", Materials Science and Engineering: A, Vol. 528, No. 12, 2011, pp. 4259-4267.
[29] B.J. Jianqiang, Kangning, S., Rui, L., Runhua, F., Sumei, W.,, "Effect of ecap pass number on mechanical properties of 2al2 al alloy", J. Wuhan Univ. Technol, Vol. No. 2008, pp. 71–74.
[30] P.R.C. R. B. Figueiredo, T. G. Langdon, "The processing of difficult-to-work alloys by ecap with an emphasis on magnesium alloys", Acta Materialia, Vol. 55, No. 2007, pp. 4769-4779.